

Characterization of Photovoltaic Modules under Arid Environments

Abubaker Younis^{1,2}, Esam Elsarrag¹, Yousef Alhorri¹ and Mahmoud Onsa²

1. Gulf Organization for Research and Development, Qatar Science and Technology Park, Tech 1 Level 2, 203, Qatar

2. Department of Mechanical Engineering, Faculty of Engineering, University of Khartoum, Khartoum, Sudan

Abstract: Performance characteristics data of solar photovoltaic (PV) cell/module are conventionally obtained under standard testing conditions. In the present work, the performance of PV modules under extreme temperatures and insulations experienced in State of Qatar was utilized to aid presenting a simplified characterization approach for the special case of arid environmental conditions. The chosen model was the well-known single diode model with both series and parallel resistors for greater accuracy. The modeling technique was validated by comparing the numerically calculated electrical characteristics with experimentally obtained data using two approaches: a single indoor fixed monocrystalline PV module inside a solar simulation chamber which physically simulated different weather scenarios by changing irradiation intensities and temperature, and a set of outdoor fixed polycrystalline PV modules. The result of the indoor experiment was presented in form of performance curves, and the outdoor experiment results in a monthly accumulated power production chart format. Both illustration types showed acceptable tolerance.

Key words: Photovoltaics, electrical characterization, mathematical modeling.

1. Introduction

A solar photovoltaic (PV) cell/module has been always defined as the semiconductor device that converts sunlight into electricity, and the modeling and simulation of its electrical behavior is common practice, and has been widely reported. In reported literature, various approaches have been employed to express the electrical behavior of solar cells/modules. Rauschenbach [1], Townsend, [2], Eckstein [3], and Schroder [4] reviewed several models and their utility for system design purposes. Single diode model for PV cell electrical behavior modeling has been studied intensively among authors [5], work was focused on single-diode model and I-V and P-V characteristics were presented in function of series resistance, parallel resistance, temperature and the irradiation. Bikaneria et al. [6] presented one diode PV cell model, the theory, the construction, and working of PV cells.

Corresponding author: Esam Elsarrag, Ph.D., professor, research fields: building and energy, renewable energy, built environment. Email: elsarrag@hotmail.com.

Elias et al. [7] developed a model for an ideal solar cell of a PV module using MATLAB software. The simulation was carried out to evaluate the influence of the variation of solar cell temperature, solar irradiation, diode ideality factor and energy gap on I-V and P-V characteristics of the PV cell. Petkov et al. [8] used classical and modified single-diode models to model the electrical behavior of PV cells while using Mathcad software. A similar approach was also used by Anku et al. [9] who introduced an optimization model to ensure efficient use of PV modules by building a single diode model using blocks from the MATLAB/Simulink library. Patel and Sharma [10] and Fares et al. [11] also depended on MATLAB/SIMULINK for modeling, simulation and implementation of the solar photovoltaic cell. The characteristics were obtained for both the single cell module and the whole PV module.

The effect of the surrounding environmental conditions was also tackled numerously in the literature with Muralidharan [12], in particular, Ref. [12] analyzed the effect of varying physical and environmental factors on the I-V characteristics of a

PV cell. Ghosh et al. [13] defined a circuit-based simulation model for a PV module to obtain the electrical behavior of a PV module with respect to changes in environmental parameters of temperature and irradiation.

In recent years, substantial progress has been made in the development of mathematical models which sufficiently describe the electrical system of PV modules. However, for the accurate prediction of the electrical behavior of PV modules, a comprehensive and precise model is of interest thus far. Particularly one which could be used in a variety of climates. This article presents a model and a solution algorithm, which can be used to characterize the performance of a PV cell/module under extreme environmental conditions of irradiation and temperature. The described approach was continually validated against experimentally obtained data to further improve the model and its accuracy.

2. Modeling and Solution Algorithm

The equivalent electrical circuit of a PV cell in the single diode model is a single diode circuit shown in Fig. 1. The circuit consists of photocurrent source, diode, shunt or parallel resistor and a series resistor in the load branch.

Then the current and voltage (I-V) characteristics of the single diode model-derived using Kirchhoff law are given by Chan et al. [14]:

$$\begin{aligned} I &= I_{ph} - I_d - I_p \\ &= I_{ph} - I_o \times \left[e^{\left(\frac{V+I \times R_s}{A \times N_s \times v_T} \right)} - 1 \right] - \frac{V + I \times R_s}{R_p} \quad (1) \end{aligned}$$

where light or photocurrent I_{ph} , diode reverse saturation current I_o , and shunt or parallel resistance R_p are unknown parameters. The respected equation for each of the three parameters is a function of cell temperature, and absorbed solar radiation.

Light current or photocurrent I_{ph} equation is a function of solar irradiation G , cell temperature T_c and short circuit current temperature coefficient μ_{sc} .

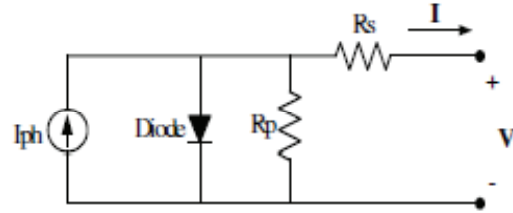


Fig. 1 The equivalent circuit of single diode model for a solar PV cell.

Then the photocurrent equation representing any operational conditions is [15]:

$$I_{ph} = \frac{G}{G_{ref}} \times [I_{ph,ref} + \mu_{sc} \times \Delta T] \quad (2)$$

where G_{ref} is reference value of solar irradiation equals to 1,000 W/m², $I_{ph,ref}$ is the photocurrent at reference conditions (Standard Testing Conditions) and it could be approximated to the reference value of the short circuit current $I_{sc,ref}$ when PV cell is short circuited according to Bellia et al. [15], then:

$$I_{ph,ref} = I_{sc,ref} \quad (3)$$

Temperature difference $\Delta T = T_c - T_{c,ref}$, where the reference temperature $T_{c,ref} = 298K$.

The well-known Diode reverse saturation current equation is according to Chan et al. [14]:

$$I_o = D \times T_c^3 \times e^{\left(\frac{-q \times \varepsilon_G}{A \times N_s \times v_T} \right)} \quad (4)$$

where D is called the diode diffusion factor and ε_G is the material band gap energy (1.11 eV for Si at 300 K [16]).

When dividing the reverse saturation current Eq. (4) by itself at STC conditions, it becomes:

$$\begin{aligned} I_o &= I_{o,ref} \times \left(\frac{T_c}{T_{c,ref}} \right)^3 \\ &\times e^{\left[\left(\frac{-q \times \varepsilon_G}{A \times N_s \times v_T} \right) \times \left(\frac{1}{T_{c,ref}} - \frac{1}{T_c} \right) \right]} \quad (5) \end{aligned}$$

Ahmad et al. [17] have introduced approximations to $I_{o,ref}$:

$$I_{o,ref} = I_{sc,ref} \times e^{\left(\frac{-V_{oc,ref}}{A \times N_s \times v_T} \right)} \quad (6)$$

Then merging Eq. (6) into Eq. (5) will result in:

$$I_o = I_{sc,ref} \times \left(\frac{T_c}{T_{c,ref}} \right)^3 \times e^{\left(\frac{-V_{oc,ref}}{A \times N_s \times v_T} \right)} \times e^{\left[\left(\frac{q \times \varepsilon_G}{A \times N_s \times v_T} \right) \times \left(\frac{1}{T_{c,ref}} - \frac{1}{T_c} \right) \right]} \quad (7)$$

A is the ideality factor and its value differs based on photovoltaic cell technology. The chosen A values for purpose of this study are 1.2 and 1.3 for monocrystalline and polycrystalline respectively by Tsai et al. [18].

N_s is the number of cells in series, v_T is called the thermal voltage and is given by the equation according to:

$$v_T = \frac{k \times T_c}{q} \quad (8)$$

And hence R_p will be:

$$R_p = \frac{V_{mp,ref} + R_s \times I_{mp,ref}}{I_{sc,ref} - I_{sc,ref} \times e^{(V_{mp,ref} + R_s \times I_{mp,ref} - V_{oc,ref})} + I_{sc,ref} \times e^{\left(\frac{-V_{oc,ref}}{A \times N_s \times v_T} \right)} - \frac{P_{max,ex}}{V_{mp,ref}}} \quad (10)$$

Electrical and thermal characteristics values are taken from manufacturer data sheet provided for RNG-50D module (50W Monocrystalline Solar Panel) demonstrated in the following tables.

Effect of temperature on the open circuit voltage, short circuit current, and the optimum operating power

$$P_{max,ex} = P_{max,ref} \times \left(1 - \mu_{mp} \times (T_c - T_{c,ref}) \right) \quad (13)$$

Then updating Eqs. (7) and (10) by Eqs. (11)-(13):

$$I_o = I_{sc} \times \left(\frac{T_c}{T_{c,ref}} \right)^3 \times e^{\left(\frac{-V_{oc}}{A \times N_s \times v_T} \right)} \times e^{\left[\left(\frac{q \times \varepsilon_G}{A \times N_s \times v_T} \right) \times \left(\frac{1}{T_{c,ref}} - \frac{1}{T_c} \right) \right]} \quad (14)$$

$$R_p = \frac{V_{mp,ref} + R_s \times I_{mp,ref}}{I_{sc} - I_{sc} \times e^{(V_{mp,ref} + R_s \times I_{mp,ref} - V_{oc})} + I_{sc} \times e^{\left(\frac{-V_{oc}}{A \times N_s \times v_T} \right)} - \frac{P_{max,ex}}{V_{mp,ref}}} \quad (15)$$

Preliminary analysis to voltage readings obtained from the experimental testing showed that voltage variation profile could be approximated to the closest known nonlinear function profile which is the natural logarithmic function.

Then the voltage generating function could be

where k is Boltzmann's constant 1.381×10^{-23} J/K and q is the electronic charge (1.602×10^{-19} coulomb). T_c is the cell temperature. Ahmad et al. [17] have suggested that the chosen value of R_p when substituted should automatically make the computed maximum power equals the experimental maximum power at its reference conditions or standard test conditions, then the next equation is:

$$\begin{aligned} I_{mp,ref} &= I_{ph,ref} - I_{o,ref} \\ &\times \left[e^{\left(\frac{V_{mp,ref} + I_{mp,ref} \times R_s}{A \times N_s \times v_T} \right)} - 1 \right] \\ &- \frac{V_{mp,ref} + R_s \times I_{mp,ref}}{R_p} \end{aligned} \quad (9)$$

has been considered by the equations:

$$V_{oc} = V_{oc,ref} \times \left(1 - \mu_{oc} \times (T_c - T_{c,ref}) \right) \quad (11)$$

$$I_{sc} = I_{sc,ref} \times \left(1 + \mu_{sc} \times (T_c - T_{c,ref}) \right) \quad (12)$$

approximated by natural logarithm function of time t :

$$V = lnt \quad (16)$$

For numerical solution simplification purposes, and due to its small magnitude compared with the parallel resistance R_p , series resistance R_s is neglected.

Table 1 Renogy's RNG-50D electrical, thermal and mechanical characteristics.

Electrical Data	
Maximum power at STC	50 W
Optimum operating voltage (V_{mp})	18.5 V
Optimum operating current (I_{mp})	2.7 A
Open circuit voltage (V_{oc})	22.7 V
Short circuit current (I_{sc})	2.84 A
Module efficiency	14.67%
Thermal characteristics	
Operating module temperature	-40 to +90
Nominal operating cell temperature (NOCT)	47 ± 2 °C
Temperature coefficient of $P_{max} (\mu_{mp})$	-0.23 %/°C
Temperature coefficient of $V_{oc} (\mu_{oc})$	-0.33 %/°C
Temperature coefficient of $I_{sc} (\mu_{sc})$	0.05 %/°C
Number of cells	36 (4 × 9)
Solar cell type	Monocrystalline

Löper et al. [19] have suggested adding a constant offset to the open circuit voltage V_{oc} as fit parameter so to obtain from the numerical solution electrical

Table 2 Solarturk energi STR60 electrical and thermal characteristics.

Electrical Data	
Maximum power at STC	250 W
Optimum operating voltage (V_{mp})	29.98 V
Optimum operating current (I_{mp})	8.34 A
Open circuit voltage (V_{oc})	37.41 V
Short circuit current (I_{sc})	8.79 A
Module efficiency	15.3%
Thermal characteristics	
Operating module temperature	-40 to +120
Nominal operating cell temperature (NOCT)	47 ± 2 °C
Temperature coefficient of $P_{max} (\mu_{mp})$	-0.43 %/°C
Temperature coefficient of $V_{oc} (\mu_{oc})$	-0.32 %/°C
Temperature coefficient of $I_{sc} (\mu_{sc})$	0.05 %/°C
Number of cells	60 (6 × 10)
Solar cell type	Polycrystalline

characteristics converging to the experimental ones. The constant offset is open circuit voltage at STC conditions $V_{oc,ref}$, then Eq. (11) will be:

$$V_{oc}^* = V_{oc,ref} \times (1 + \mu_{oc} \times (T_c - T_{c,ref})) \quad (11)^*$$

Updating Eqs. (14) and (15) by Eq. (11)*, the new statement of the diode reverse saturation current I_o is:

$$I_o = I_{sc} \times \left(\frac{T_c}{T_{c,ref}} \right)^3 \times e^{\left(\frac{-V_{oc}^*}{A \times N_s \times v_T} \right)} \times e^{\left[\left(\frac{q \times \varepsilon_G}{A \times N_s \times v_T} \right) \times \left(\frac{1}{T_{c,ref}} - \frac{1}{T_c} \right) \right]} \quad (14)^*$$

And for the resistance in parallel:

$$R_p = \frac{V_{mp,ref} + R_s \times I_{mp,ref}}{I_{sc} - I_{sc} \times e^{(V_{mp,ref} + R_s \times I_{mp,ref} - V_{oc}^*)} + I_{sc} \times e^{\left(\frac{-V_{oc}^*}{A \times N_s \times v_T} \right)} - \frac{P_{max,ex}}{V_{mp,ref}}} \quad (15)^*$$

Numerical solution for the implicit nonlinear I-V characteristics Eq. (1) is of interest, so to compute the relevant unknown parameters and then to evaluate current and voltage characteristics.

The numerical solver used here is a combination of bisection, secant and inverse quadratic interpolation methods, coded in MATLAB software by the command FZERO Mathworks (2016).

The equations' solving pattern or solution algorithm used to numerically compute I-V characteristics is then translated to MATLAB command lines which displays results in form of figures and graphs. Fig. 2

demonstrates the solution algorithm flow chart.

3. Test Setup and Procedure

3.1 Indoor Setup

A solar/weather simulation chamber, which is a controlled environment is used for characterization of the PV module and validation of the numerical solution results.

The testing was conducted in an *Atlas SEC 1100 Solar Simulator Chamber* located in GORD's research facility (TechnoHub) at Qatar. The SEC 1100 has a chamber size of 1,100 liters with an effective radiation

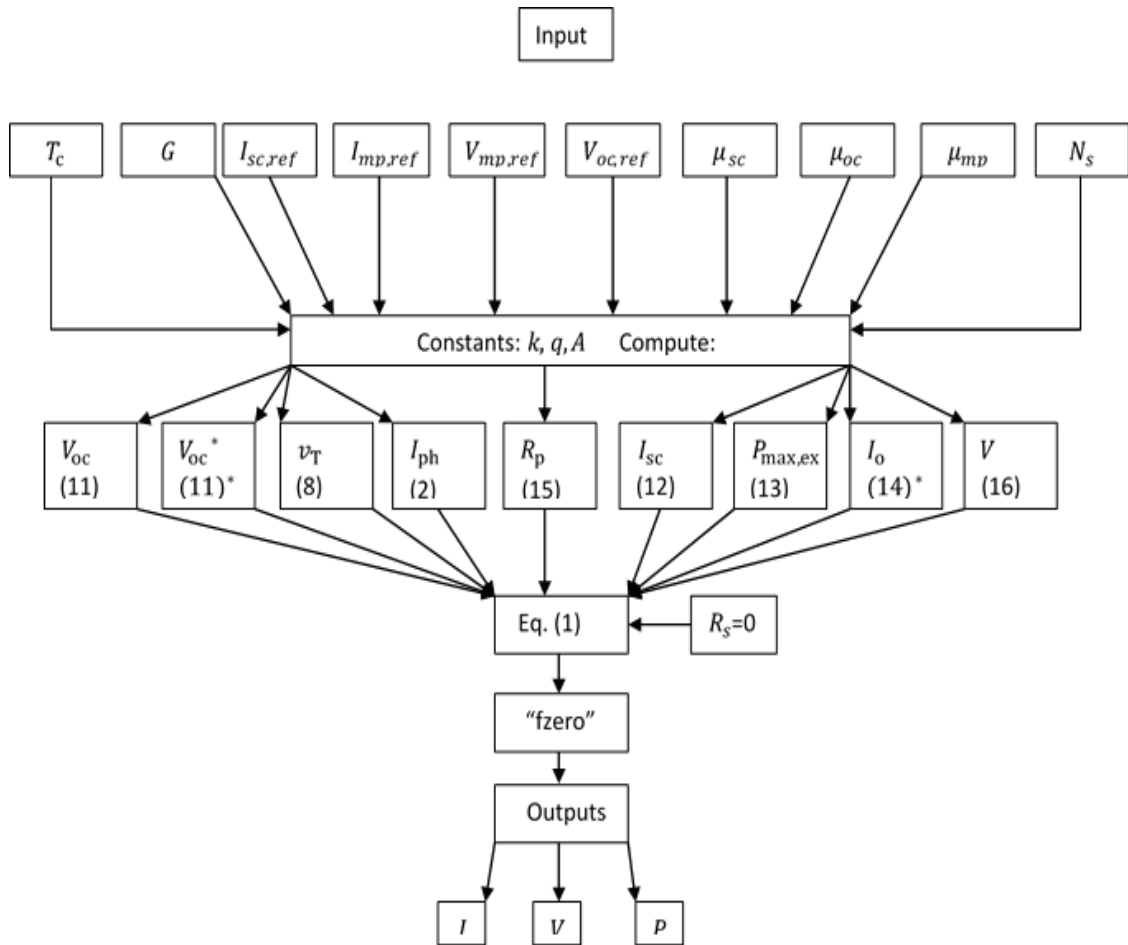


Fig. 2 Flow chart demonstrates the solution sequence of the single diode model to obtain electrical characteristics.

area of 5,600 cm² and acts as a perfect test chamber to characterize small to medium sized PV panels. The integrated Metal Halide Global (MHG Model: 4,000 W Luminary) conforms with IEC 60904 Class A guidelines and provides quality solar simulation with a close spectral match to natural sunlight combined with high irradiation efficiency and spatial uniformity in the test area. The MHG lamp provides adjustable output up to a maximum of 1,200 W/m² with a spectral range of 280-3,000 nm.

The parameters that can be controlled in the chamber include air (ambient) temperature, irradiation, relative humidity via a touch screen control panel located on the front of the chamber. The device also has logging capabilities for these parameters along with a 6 channel DAQ for temperature sensors, irradiation measurement and Black Standard Temperature control

in real time. The output is saved in csv format as well as displayed on screen graphically. Multi-stage safety features ensure that the chamber operates in the preset limits and ensure prolonged testing durations.

The response of the PV at two different irradiation levels (700 W/m² & 1,200 W/m²) of the sun was tested. In each set of irradiation values, the temperature of the chamber was varied to achieve different operating temperatures for the PV module, thus dividing the test to multiple tests with different combinations of Irradiation and PV Temperatures. Each test consisted of measuring the open circuit voltage V_{oc} , short circuit current I_{sc} and output parameters (voltage & current) of the PV at varying load resistances ranging from 1 Ohm to 100 Ohm.

The load resistance was simulated using 50 W power resistors of values 1 Ohm, 4 Ohm and 8 Ohm with

multiple resistors being connected together in series combinations via a custom-made micro-controller based relay network to achieve different progressive resistive values from 1 to 100 Ohm in steps of 1 Ohm. The output of the PV was measured for consistency by keeping each value of resistance constant for 5 minutes under the same conditions. The value was limited at 100 Ohm due to the reason that the PV performance degraded exponentially after the 10 Ohm mark and adding more resistance was not relevant to the test which was trying to validate a model which predicts a practical scenario, where the maximum possible resistance values would not go beyond a dozen or so ohms.

The temperature of the PV was monitored at 6 different points of the PV backside and the average temperature was considered as the PV temperature. The measurement was done by Class B PT 100 temperature sensors connected to the monitoring system of the Atlas SEC 1100 solar simulator chamber logger which gave out real time outputs of the parameters being monitored except the power output of the PVs. Fig. 3 shows the monocrystalline PV inside the simulator and the PT100 sensors attached at its backside. The power output of the PV was measured using a separate micro-controller based system linked to the resistance simulator and used an ACS712ELECTR-05B-T based current sensor and voltage divider coupled with 10 bit ADC of the microboard, which provided resolutions of 0.009 A for the current and 0.005 V for the voltage. The data were logged in a csv file format for analysis and the power curves obtained at different test parameters were validated against the simulated curves from the model. The humidity was set constant at 30%.

The irradiation at the plane of the PV panel was measured using an ISO 9060 first class compliant Kipp & Zonen CMP 6 pyranometer (in the SEC) which can measure up to 2,000 W/m² in a spectral range of 285 to 2,800 nanometers with a sensitivity of 12.29×10^{-6} $\mu\text{V}/\text{W}\cdot\text{m}^2$ and a 180° field of view. Fig. 4 summarizes

the schematic diagram of the full setup.

3.2 Outdoor Setup

A set of four 250 W Polycrystalline PV modules was mounted outdoor in the GORD TechnoHub research facility. Fig. 5 photographically demonstrates the setup. The monitoring and logging of the electrical characteristics were done by designing and building a custom-made microcontroller based Smart Data Logging system which measured each parameter with specific sensors. The logging was done in real time high frequency samples and saved to a memory card in CSV format for easy analysis. The current was measured using ACS712 based current sensors, which can measure DC current in both directions with a range of 20 Amps, and an accuracy of 1.5%. The recording and monitoring was done automatically by the logger and the data were saved in a memory card with all information per day saved in one file with the date and timestamp. The recording was done from sunrise to sunset using the RTC information and was turned on during the day and off during the night. The weather data for the year of 2017 were collected using weather station fixed in the same research facility.

4. Results and Discussions

The following set of figures present many selected current vs. voltage (I-V) and power vs. voltage (P-V) curves, which compare experimental characteristics belonging to indoor test with the simulated characteristics. The values of temperatures and irradiation intensities are determined randomly according to suitability and availabilities at the testing facility. Graphs are generated by MATLAB software.

The process of validating the new model results against the experimentally obtained results is visually demonstrated in Figs. 6 and 7 which present data in I-V curve format. A decent identicity between the validation and simulation curves is observed, also the difference in magnitude of short circuit current between the two cases is barely distinguishable.

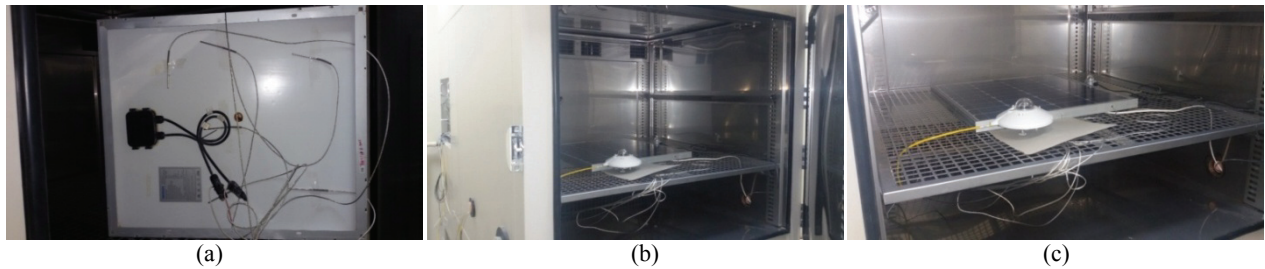


Fig. 3 Photographic views of RNG-50 PV module placed inside the solar simulator and the PT100 sensors are attached to its backside.

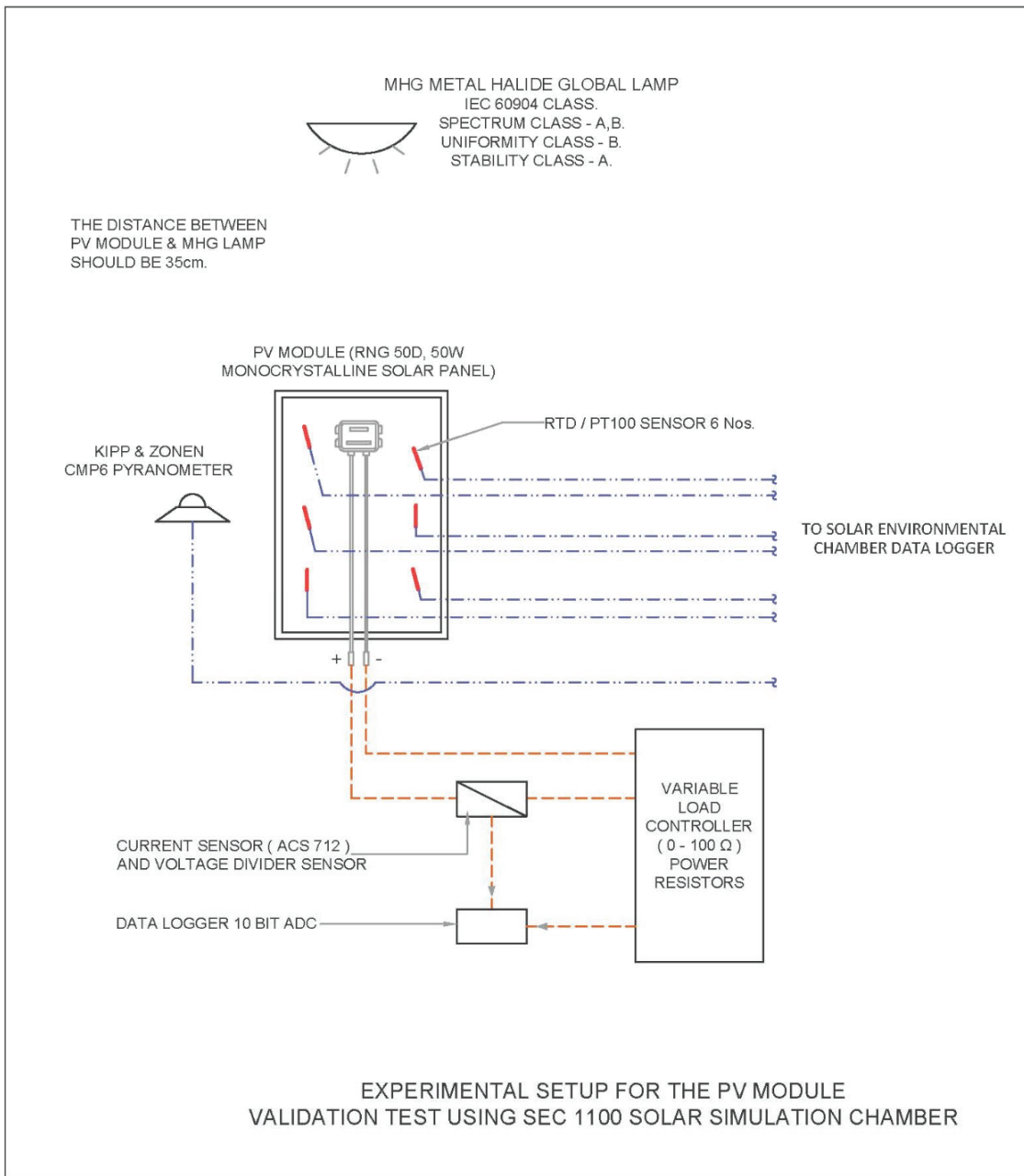


Fig. 4 Schematic diagram for the PV module testing setup at GORD's Technohub.



Fig. 5 Photographic view of outdoor setup for testing polycrystalline PV module at GORD's Technohub.

Complying with the I-V figures trend, Figs. 8 and 9 show almost identical simulation and validation curves

for the pre- and post- maxima region, while a non-drastic displacement between the two curves occurred at the maxima region. It is also clearly illustrated that the precision of the results is within an acceptable range, although further considerations would be of interest to maximize the model accuracy, so when including other environmental parameters there would be no effect on the total tolerance percentage.

Typical P-V behavior of the PV cell/module was maintained as illustrated in Figs. 10-12, which show performance curves generated from the new model following the same trend of the conventional theoretical curves with wider range of temperatures and fixed

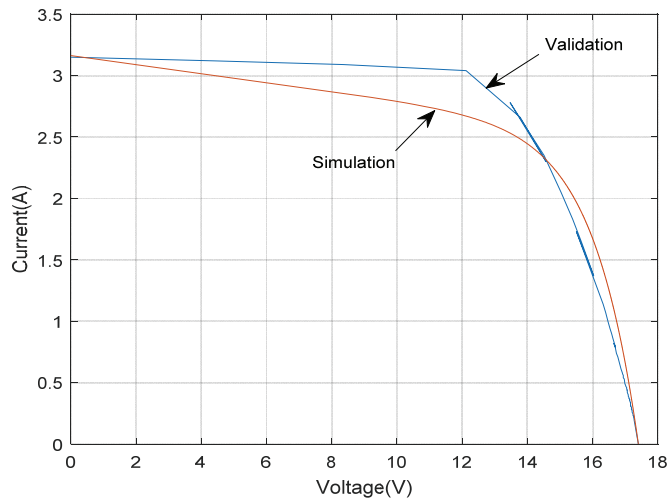


Fig. 6 Current vs. voltage at 95 °C and 1,100 W/m².

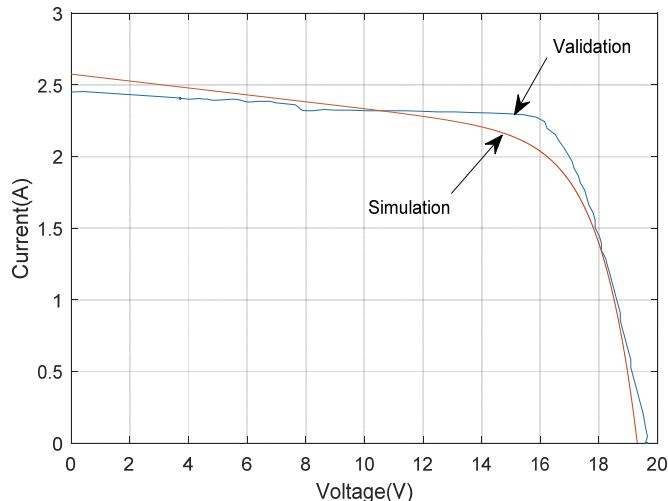


Fig. 7 Current vs. voltage at 66 °C and 900 W/m².

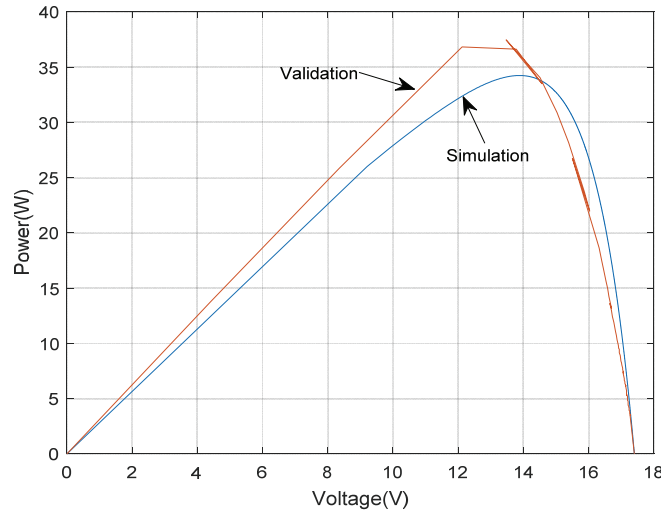


Fig. 8 Power vs. voltage at 95 °C and 1,100 W/m².

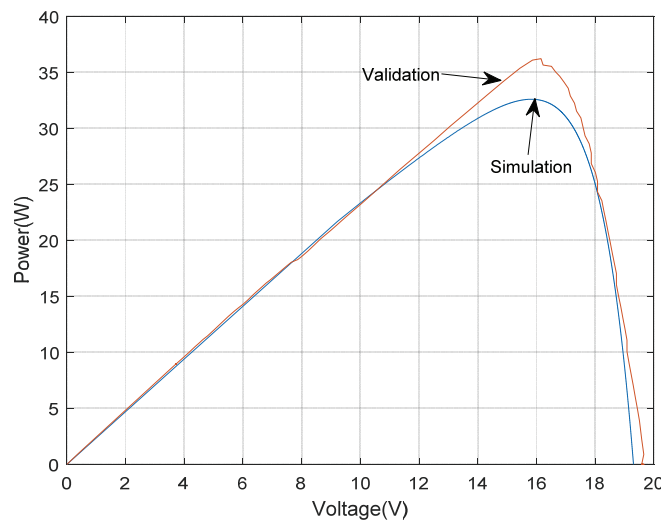


Fig. 9 Power vs. voltage at 66 °C and 900 W/m².

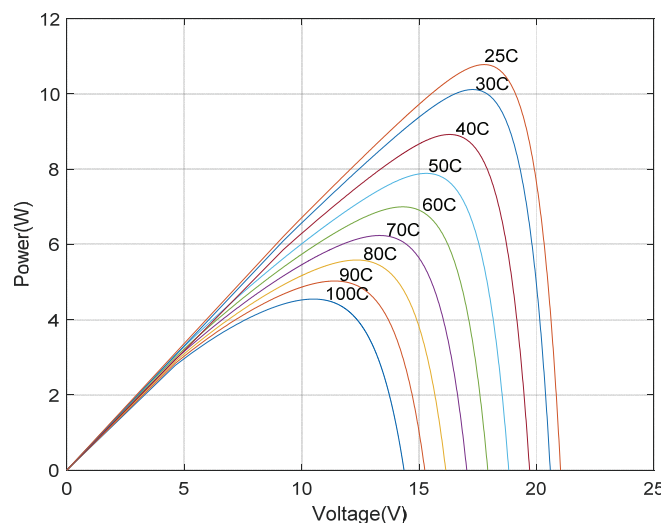


Fig. 10 Power vs. voltage at different temperatures and 250 W/m².

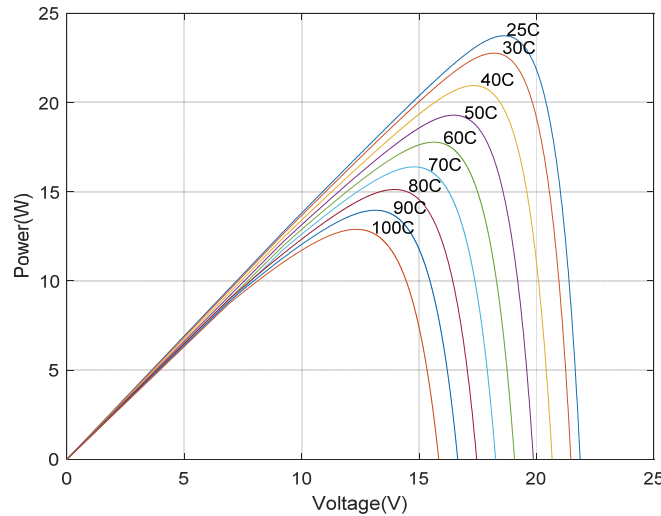


Fig. 11 Power vs. voltage at different temperatures and 500 W/m^2 .

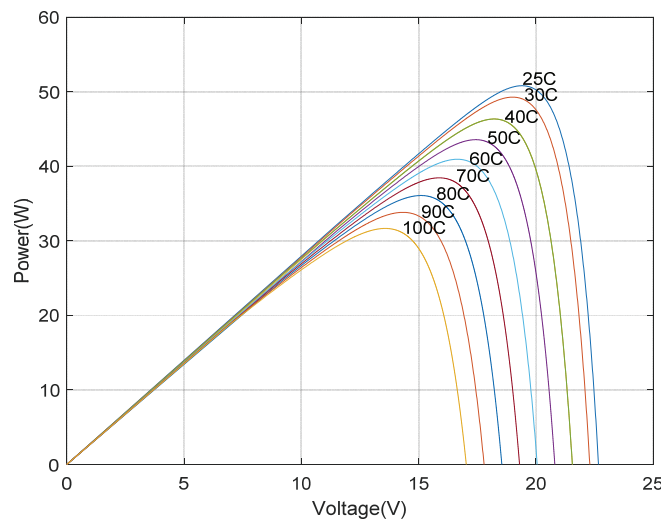


Fig. 12 Power vs. voltage at different temperatures and $1,000 \text{ W/m}^2$.

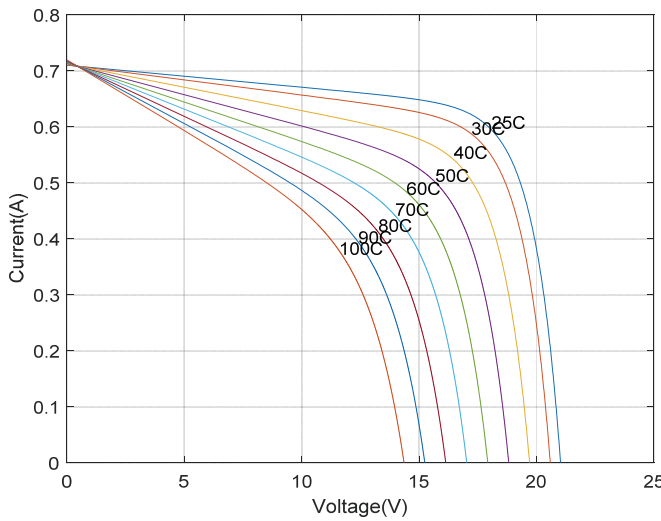


Fig. 13 Current vs. voltage at different temperatures and 500 W/m^2 .

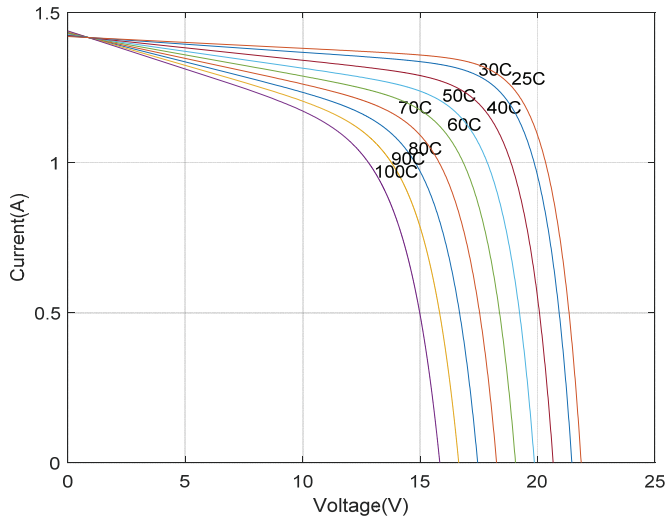


Fig. 14 Current vs. voltage at different temperatures and 250 W/m^2 .

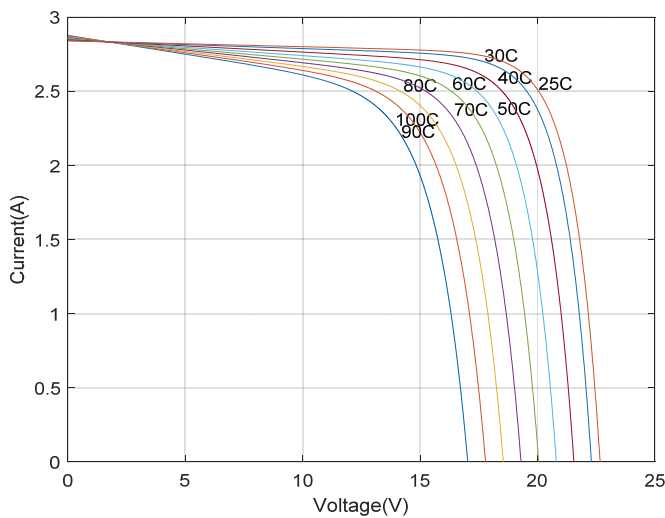


Fig. 15 Current vs. voltage at different temperatures and $1,000 \text{ W/m}^2$.

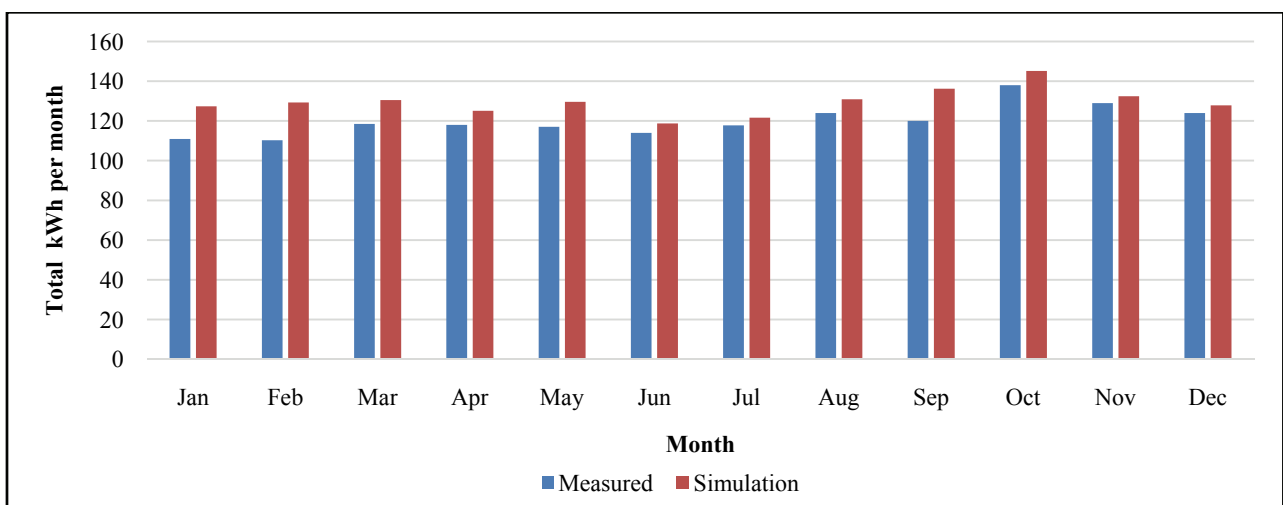


Fig. 16 Total power produced by 4 polycrystalline PV modules in GORD's Technohub for 2017.

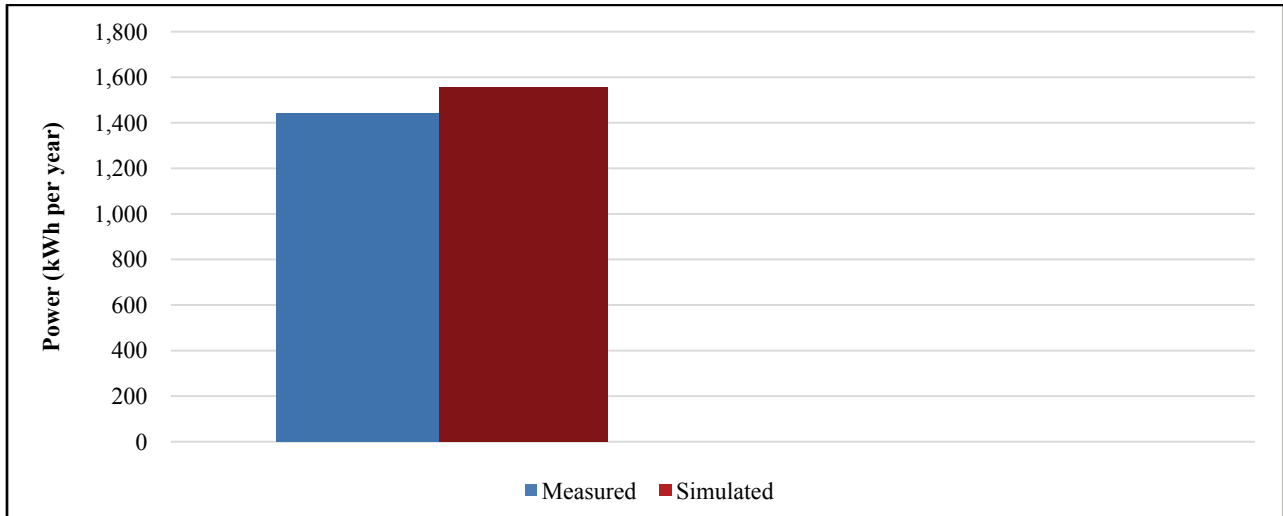


Fig. 17 Annual measured power production compared with the simulated power for the polycrystalline PV set in the year 2017.

irradiance. The effect of temperature demonstrated in the previous figures complies with the governing mathematical equations which explicitly include temperature terms that by its turn, reduce proportionally the open circuit voltage and the maximum output power with the temperature increase.

As the mentioned typicality of P-V curves also implies on the computationally generated I-V performances charts in Figs. 13-15, it is distinctly presented that the temperature has almost no effect on the short circuit current magnitude and that perfectly matches the literature.

The real-life applicability of the visualized convergence in the corresponding curves presented earlier was tested by using the outdoor setup data collected for the year of 2017. Fig. 16 shows bar chart of the monthly accumulated power produced by the 4 PV panels drawn against the simulated power production.

As shown in Fig. 17 the difference between annual simulated and measured power performance rests within acceptable range of exactly 8%.

5. Conclusions

The I-V and P-V characteristics resulted from the numerical solution of the electrical model presented in this work were validated against experimentally

obtained data from both monocrystalline and polycrystalline PV modules placed indoor and outdoor respectively at multiple combinations of the input parameters the model could accept, namely, the irradiance and temperature. The presented graphs have shown sufficient convergence and very acceptable for non-delicate applications of the PV panels, annual-wise the prediction capability of the modeling method was responsive as it clearly takes in consideration the heat and light intensity effects. Hence the model and the solution algorithm could be described as reliable ones.

References

- [1] Rauschenbach, S. 1980. *Solar Cell Array Design Handbook—The Principle Technology of Photovoltaic Energy Conversion*.
- [2] Townsend, T. U. 1989. “A Method for Estimating the Long-Term Performance of Direct-Coupled Photovoltaic Systems.” MS Thesis. doi:10.1016/0038-092X(84)90010-0.
- [3] Eckstein, J. 1990. “Detailed Modelling of Photovoltaic System Components.” MS Thesis.
- [4] Schroder, D. K. 2006. *Material and Device Semiconductor Material and Device*. 3rd ed. Physics Today. doi:10.1063/1.2810086.
- [5] Azzouzi, M., Popescu, D., and Bouchahdane, M. 2016. “Modeling of Electrical Characteristics of Photovoltaic Cell Considering Single-Diode Model.” *Journal of Clean Energy Technologies* 4 (6): 414-20.

- doi:10.18178/JOCET.2016.4.6.323.
- [6] Bikaneria, J., Prakash Joshi, S., and Joshi, A. 2013. "Modeling and Simulation of PV Cell Using One-Diode Model." *International Journal of Scientific and Research Publications* 3 (10): 2250-3153.
- [7] Elias, B. H., AlSadoon, S. H. M., and Abdulgafar, S. A. 2014. "Modeling and Simulation of Photovoltaic Module Considering an Ideal Solar Cell." *International Journal of Advanced Research in Physical Science* 1 (August): 9-18.
- [8] Petkov, M., Markova, D., and Platikanov, S. 2011. Modelling of Electrical Characteristics of 2. doi:10.5767/anurs.cmat.110202.en.171P.
- [9] Anku, N. E. L., Kankam, A., Takyi, A., and Ampsonah, R. 2015. "A Model for Photovoltaic Module Optimisation." *Journal of Mechanical Engineering and Automation* 5 (2): 72-9. doi:10.5923/j.jmea.20150502.02.
- [10] Patel, J., and Sharma, G. 2013. "Modeling and Simulation of Solar Photovoltaic Module Using Matlab/Simulink." *International Journal of Research in Engineering Technology* 2 (3): 225-8.
- [11] Fares, M. A., Atik, L., Bachir, G., and Aillerie, M. 2017. "Photovoltaic Panels Characterization and Experimental Testing." *Energy Procedia* 119 (July): 945-52. doi:10.1016/j.egypro.2017.07.127.
- [12] Muralidharan, R. 2014. "Mathematical Modeling, Simulation and Validation of Photovoltaic Cells." *International Journal of Research in Engineering and Technology* 3 (10): 170-4.
- [13] Ghosh, S., Shawon, M., Rahman, A., and Abdullah, R. 2013. "Modeling of PV Array and Analysis of Different Parameters." *International Journal of Advancements in Research & Technology* 2 (5): 358-63.
- [14] Chan, D. S. H., Phillips, J. R., and Phang, J. C. H. 1986. "A Comparative Study of Extraction Methods for Solar Cell Model Parameters." *Solid-State Electronics* 29 (3): 329-37. doi:10.1016/0038-1101(86)90212-1.
- [15] Bellia, H., Youcef, R., and Fatima, M. 2014. "A Detailed Modeling of Photovoltaic Module Using MATLAB." *NRIAG Journal of Astronomy and Geophysics* 3 (1): 53-61. doi:10.1016/j.nrjag.2014.04.001.
- [16] Kittel, C. 2005. *Introduction to Solid State Physics*, 8th ed. New York: John Wiley.
- [17] Ahmad, T., Sobhan, S., and Nayan, F. 2016. "Comparative Analysis between Single Diode and Double Diode Model of PV Cell: Concentrate Different Parameters Effect on Its Efficiency." *Journal of Power and Energy Engineering* 4 (3): 31-46. doi:10.4236/jpee.2016.43004.
- [18] Tsai, H., Tu, C., and Su, Y. 2008. "Development of Generalized Photovoltaic Model Using MATLAB/SIMULINK." Proceedings of the World Congress on Engineering and Computer Science 2008 (WCECS 2008), October 22-24, 2008, San Francisco, USA.
- [19] Löper, P., Pysch, D., Richter, A., Hermle, M., Janz, S., Zacharias, M., and Glunz, S. W. 2012. "Analysis of the Temperature Dependence of the Open-Circuit Voltage." *Energy Procedia* 27: 135-42. doi:10.1016/j.egypro.2012.07.041.